Advances in Aerospace Science and Technology, 2023, 8, 34-54
https://www.scirp.org/journal/aast
ISSN Online: 2473-6724
ISSN Print: 2473-6708

Solar Wind Interaction with Jupiter's Magnetosphere

Jenny Marcela Rodríguez-Gómez[1,2]

[1]NASA Goddard Space Flight Center, Greenbelt, USA
[2]Physics Department, The Catholic University of America, Washington DC, USA
Email: rodriguezgomez@cua.edu, jenny.m.rodriguezgomez@nasa.gov

How to cite this paper: Rodríguez-Gómez, J.M. (2023) Solar Wind Interaction with Jupiter's Magnetosphere. *Advances in Aerospace Science and Technology*, **8**, 34-54.
https://doi.org/10.4236/aast.2023.83004

Received: June 23, 2023
Accepted: September 10, 2023
Published: September 13, 2023

Abstract

This paper studies the effects of the solar wind on Jupiter's magnetosphere. The solar wind parameters are characterized using the Michigan Solar Wind Model (mSWiM) solar wind data propagated to Jupiter from 1997 to 2016. This analysis covers almost solar cycles 23 and 24. Interplanetary fast shocks: Forward shocks (FS), Reverse shocks (RS), and solar wind dynamic pressure were obtained and analyzed during the apparent opposition periods. The fast forward (FS) shocks were predominant during this period. Generally, the solar wind dynamic pressure from FS and RS shocks follows the solar cycles 23 and 24.

Keywords

Solar Wind, Interplanetary Fast Shocks, Magnetospheres

1. Introduction

The Solar wind originates from the Coronal Holes (CHs) associated with open field lines, the fast coronal wind is associated with them in the polar regions with speeds varying between 700 - 800 km/s and slow solar wind is associated with the CHs located in the equatorial regions with speeds ~400 km/s. The solar wind expands continuously in interplanetary space and its interaction with the planetary magnetic field creates the planetary magnetospheres. In general, the magnetosphere size is determined by the balance between solar wind dynamic pressure and the magnetic field planetary pressure (Rodríguez-Gómez, 2021 [1] and references therein).

Jupiter has a magnetic field ten times higher than the Earth's magnetic field, as result its magnetosphere reaches 150 R_J (R_J = 71,492 km) and its radiation belts are the strongest in the solar system (Plainaki *et al.* 2016 [2], Bunce *et al.*

2004 [3]).

The solar wind interaction with Jupiter's magnetosphere is still under debate (e.g., Cowley *et al.* 2008 [4]; McComas & Bagenal, 2007 [5]). But observations and theory suggest that is quite different from the Earth's magnetosphere because of the large spatial scales, rapid planetary rotation, and plasma sources in the magnetosphere (Vogt *et al.* 2019 [6]). The first studies of the Jovian magnetosphere started in the seventies, e.g., Brice and Ioannidis, 1970 [7], who applied ideas from the terrestrial magnetosphere to Jupiter. They point out that the strong magnetic field of Jupiter dominates the magnetopause, making a rotation-dominated Jovian magnetosphere. By the early 1980s was clear that the Jovian magnetosphere is dominated by an internal source—the Io torus rather than the planet's atmosphere (Delamere and Bagenal, 2010 [8]).

The relationship between auroral radio emissions and solar wind interaction with Jupiter's magnetosphere is not trivial. Observations consistently show that solar wind interactions and aurorae brightness are positively correlated at Jupiter (Badman *et al.* 2016 [9]; Dunn *et al.* 2016 [10]; Panchenko *et al.* 2013 [11]; Hess *et al.* 2012 [12]; Echer *et al.* 2010 [13]; Nichols *et al.* 2009 [14]). Additionally, Chané *et al.* 2017 [15] show their simulations agree with observations, which consistently show that solar wind perturbations and aurora brightness are positively correlated.

The solar wind power on the magnetospheric cross section is the primary energy source of auroral radio emissions, except for those of the Io-Jupiter system (Zarka, P. 1998 [16]). In general, Jovian Auroral Radio Emissions (AREs) have three main components: first the broadband kilometer component (bKOM) between ~10 and > 300 kHz, second the hectometer component (HOM) from 300 kHz to a few MHz (peaking about 800 kHz) and third the decameter components, up to 40 MHz. A component is related to the satellite Io (Io-DAM) and another component is independent of Io. It is called non-Io-DAM characterized by the high-frequency extent of HOM emission.

Magnetospheric observations are now available from some spacecraft missions one of the most important is the Galileo orbiter from 1996 to 2003, but in most cases near Jupiter upstream solar wind measurements are unavailable (Vogt *et al.* 2019 [6]). This paper aims to study the solar wind's influence on Jupiter's magnetosphere using mSWiM solar wind data propagated to Jupiter. For this purpose, we calculate the Interplanetary fast shocks: Forward shocks (FS), Reverse shocks (RS), and solar wind dynamic pressure.

2. Data

Michigan Solar Wind Model

Solar wind data propagated to Jupiter's orbit will be obtained from the one-dimensional numerical magneto hydrodynamic (MHD) code developed by the University of Michigan (Zieger and Hansen 2008 [17]). mSWiM is a 1.5-D ideal MHD model implemented with the Versatile Advection Code (VAC), a general software package designed to solve MHD equations in conservative form (Tóth, G. 1996 [18]). The model propagates the solar wind plasma radially outward from the Earth's orbit at a selected longitude in the inertial frame of reference, assuming spherical symmetry.

The simulation uses solar wind conditions measured at Earth as the inner boundary. For the solar wind predictions, it uses hourly solar wind plasma and interplanetary magnetic field (IMF) data in the RTN coordinate system from the OMNIWeb database[1] as input. This solution is then mapped to the body of interest, in this case Jupiter, to provide the predicted solar wind conditions. mSWiM has been extensively validated statistically using 12 years of Pioneer, Voyager, Ulysses, and Cassini data from 3.5 to 10 AU. Also, it was able to capture the propagation of transient events like interplanetary coronal mass ejections (ICMEs) even at solar maximum, when the corona is far from the steady state (Zieger and Hansen, 2008 [17]).

3. Interplanetary Fast Shocks

Jupiter's magnetosphere, in part is sensitive to the solar wind dynamic pressure variations. Several observations showed that aurora and radio emissions are intensified during higher solar wind pressure or induced by interplanetary shocks (Hess *et al.* 2012 [12]). ICMEs or CIRS drive interplanetary shocks. The fast forward (FS) shock is caused by ICMEs that originated from CMEs. However, when CHs are evolving, fast streams emanate, and intercept the ambient solar wind. This interaction forms a compression region between the high-speed stream and slow-speed stream; it is limited by fast forward (FS) and fast reverse (RS) shocks (Hess, S. *et al.* 2014 [19]).

The interplanetary fast shocks were identified on mSWim data using the characteristics described by Echer *et al.* 2010 [13] and Echer 2019 [20]. Those shocks are described as follows:

- Fast forward shock (FS) occurs when the solar wind speed $v_m(\text{km/s})$, density $N(\text{cm}^{-3})$, temperature $T(K)$ and magnetic field magnitude $B_m(nT)$ increase in time.
- Fast reverse shock (RS) is characterized by an increase on solar wind speed with time, while other parameters such as temperature, density, and magnetic field magnitude decrease.

The magnetic field components were obtained from mSWim model. Specifically, the magnetic field magnitude $B_m(nT)$ was obtained as

$$B_m = \sqrt{B_r^2 + B_t^2 + B_n^2} \quad (1)$$

The velocity magnitude $v_m(\text{km/s})$ of solar wind were obtained from the mSWim model.

$$v_m = \sqrt{v_r^2 + v_t^2 + v_n^2} \quad (2)$$

[1] http://omniweb.gsfc.nasa.gov/.

where subscripts *r*, *t*, *n*, indicate magnetic field and velocity components.

Γ_B, Γ_N, and v_m were calculated, where $\Gamma_B = \frac{B_2}{B_1}$ and, $\Gamma_N = \frac{N_2}{N_1}$, B_2 and N_2 are the magnetic field and density after shock. B_1 and N_1 are the magnetic field and density before the shock (see **Appendix 2**).

This work selected the apparent opposition periods from 1997 to 2016. This period is defined as the time of opposition of Earth and a given planet, in this case, Jupiter or any other body plus the solar wind propagation time from Earth to the body at an average speed of 500 km/s. The most reliable predictions are expected within 75 days of apparent opposition (**Figure 1**).

The Interplanetary fast shocks: Forward shocks (FS), and Reverse shocks (RS) were obtained in opposition periods with Jupyter. A period ± 50 days was selected before and after apparent opposition day (**Table 1**).

4. Results

± 50 days from the apparent opposition were used in this analysis. The fast shocks from 1997 to 2016 were obtained and analyzed. **Figure 2** and **Figure 3** show some examples of the detection of interplanetary shocks during the opposition periods. This procedure was applied in all periods described in **Table 1**. Their respective figures and details are summarized in **Appendix 1** and **Appendix 2**. An analysis of the dynamic pressure in each apparent opposition period was performed (Section 4.1), as well as the mean dynamic pressure variations in time from 1997 to 2016.

Dynamic Pressure Analysis

The solar wind dynamic pressure was calculated as $P_{sw} = m_p v_{sw}^2$, where m_p is the proton mass, N is the density and v_{sw} is the solar wind speed. The pressure variation is dominated by the density and solar wind speed variation. Each FS and RS shocks, $P_{sw}(nPa)$ were calculated at an initial and final point, and their variation was obtained as $\Delta P_{sw} = P_{swf} - P_{swi}$.

Figures 4-7 show the dynamic pressure distribution in FS and RS during the opposition periods from 1997 to 2016. The dotted red line denotes the mean value in each distribution. **Figure 8** summarizes the mean dynamic pressure (P_{sw}) value in time. Dotted vertical lines mark the maximum of solar cycle 23 and 24 and the minimum between both solar cycles. Those intervals were defined previously by Rodríguez-Gómez *et al.* 2020 [21], e.g., maximum of solar cycles 23 from 1999 to 2003, maximum of solar cycle 24 from 2011 to 2015, and solar minimum from 2006 to 2010.

5. Discussion

The role of the solar wind in Jupiter's magnetosphere is an open question, specifically how it influences the topology and dynamics (Ebert *et al.* 2014 [22] and references therein). The main results of this study focused on the solar wind interaction in Jupiter's magnetosphere can be summarized as follows.

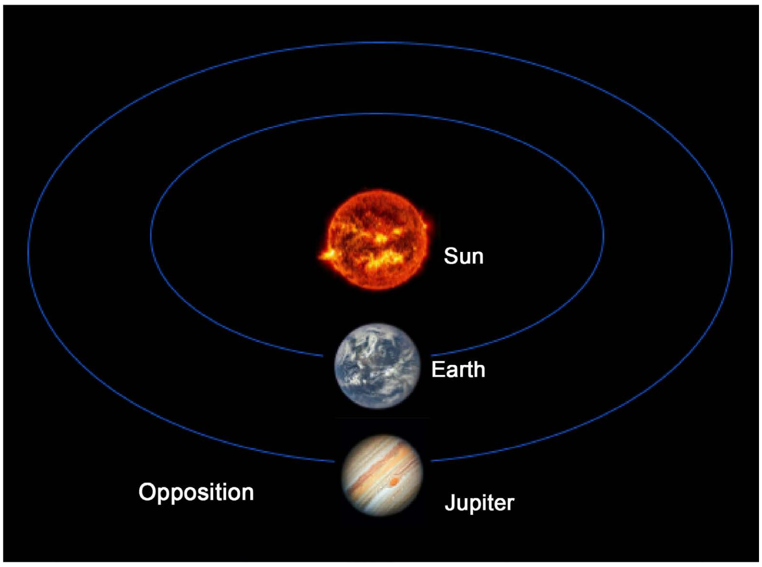

Figure 1. Apparent opposition Sun[2], Earth[3] and Jupiter[4].

Table 1. Apparent opposition periods from 1997 to 2016.

Year	Day of apparent opposition	±50 days DOY	±50 days Date
1997	234	184-284	July 3 to October 11
1998	271	221-321	August 9 to November 17
1999	309	259-359	September 16 to December 25
2000	346	296-31	October 22, 2000, to January 31, 2001
2002	14	330-64	November 26, 2001, to March 5, 2002
2004	78	28-128	January 28 to May 7
2005	108	58-158	February 27 to June 7
2006	138	88-188	March 29 to July 7
2007	170	120-220	April 30 to August 8
2008	204	150-254	May 29 to September 10
2009	239	189-289	July 8 to October 16
2010	277	227-327	August 15 to November 23
2011	314	264-364	September 21 to December 30
2012	351	301-35	October 27, 2012, to February 4, 2013
2014	19	335-69	December 1, 2013, to March 10, 2014
2015	51	1-101	January 1 to April 11
2016	82	32-99[5]	February 1 to April 8

[2]https://spaceplace.nasa.gov/gallery-sun/en/.
[3]https://www.nasa.gov/image-feature/nasa-captures-epic-earth-image.
[4]https://solarsystem.nasa.gov/resources/2486/hubbles-new-portrait-of-jupiter/.
[5]No more available data.

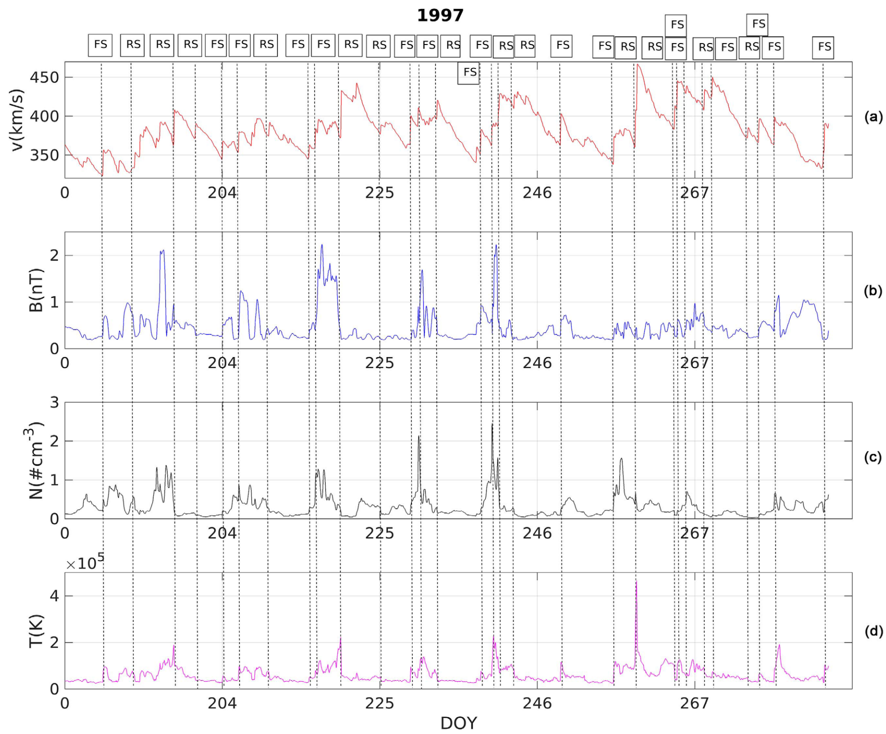

Figure 2. Solar wind data from mSWim from 184 to 284 DOY 1997. From upper to lower panel: (a) solar wind speed (v), (b) bmagnetic field magnitude (B), (c) density (N), and (d) Temperature (T). Dotted vertical lines indicate the interplanetary shocks FS and RS.

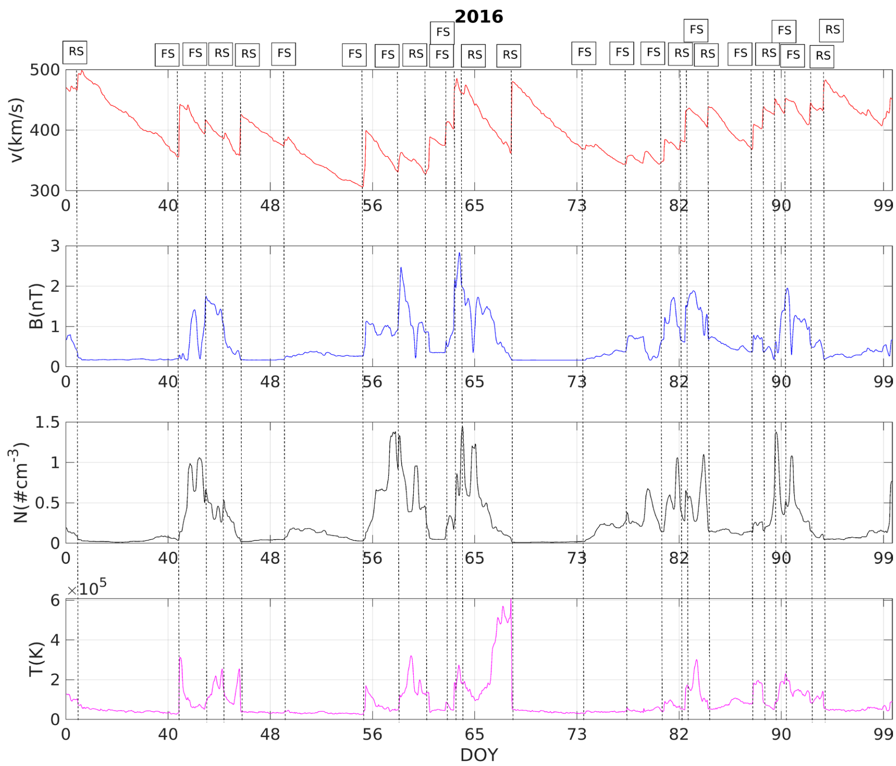

Figure 3. Solar wind data from mSWim from 32 to 99 DOY 2016. From upper to lower panel: solar wind speed (v), magnetic field magnitude (B), density (N) and Temperature (T). Dotted vertical lines indicate the interplanetary shocks FS and RS.

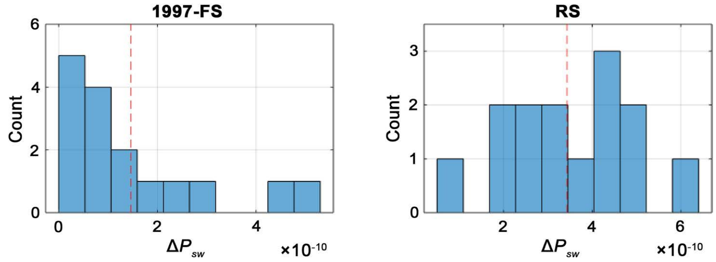

(a)

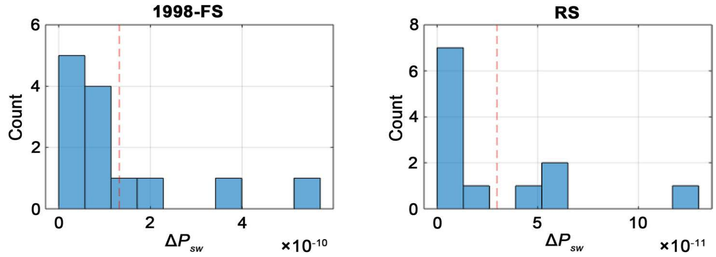

(b)

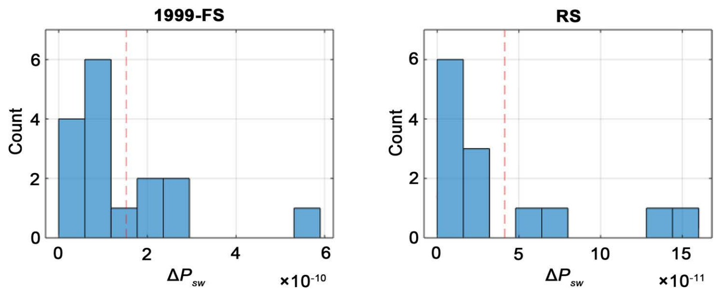

(c)

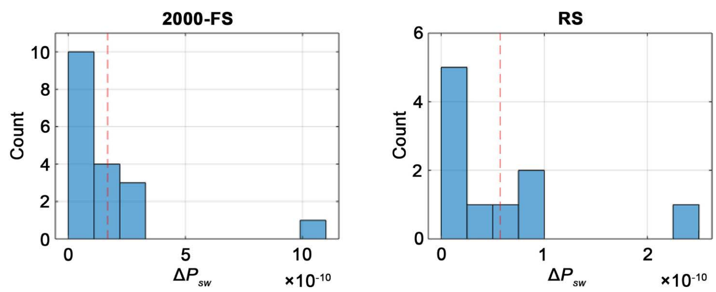

(d)

Figure 4. Dynamic pressure analysis from 1997 to 2000. Histograms of ΔP_{sw} in FS and RS shocks, the red dotted line shows the mean value in each distribution.

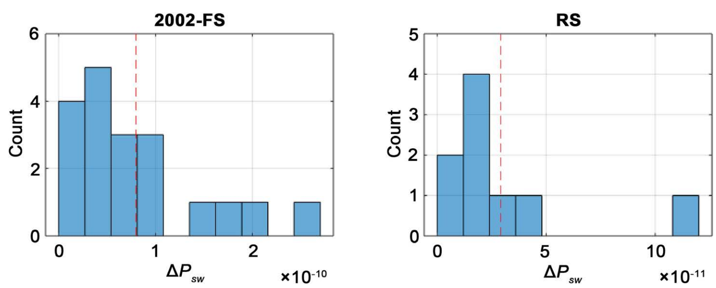

(a)

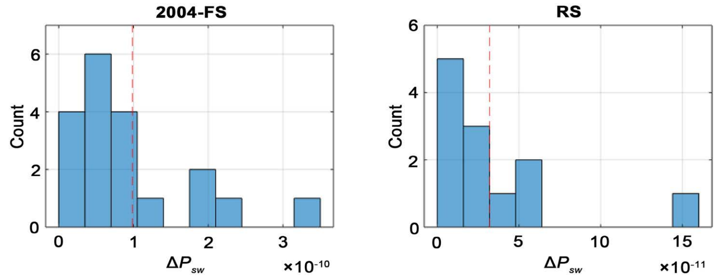

(b)

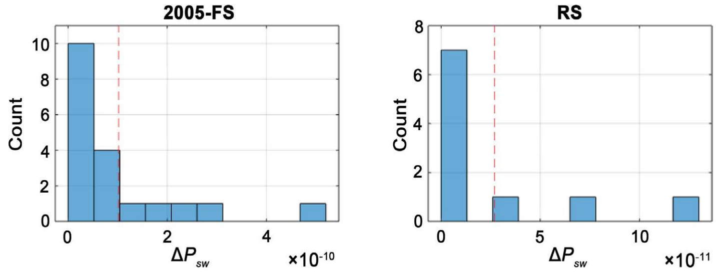

(c)

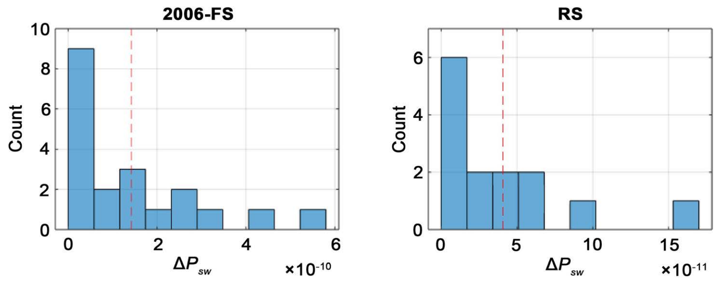

(d)

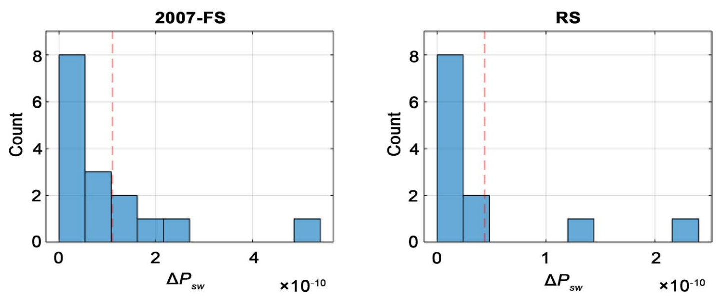

(e)

Figure 5. Dynamic pressure analysis from 2002 to 2007. Histograms of ΔP_{sw} in FS and RS shocks, the red dotted line shows the mean value in each distribution.

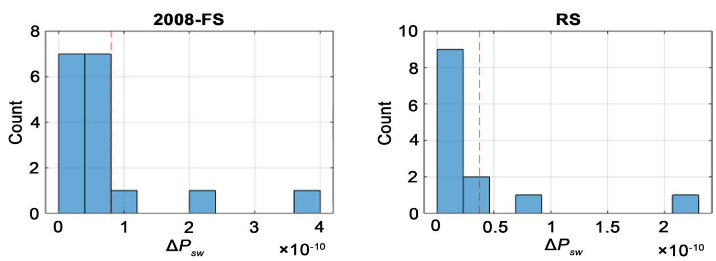

(a)

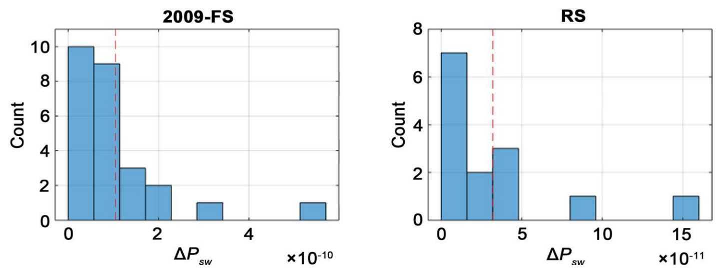

(b)

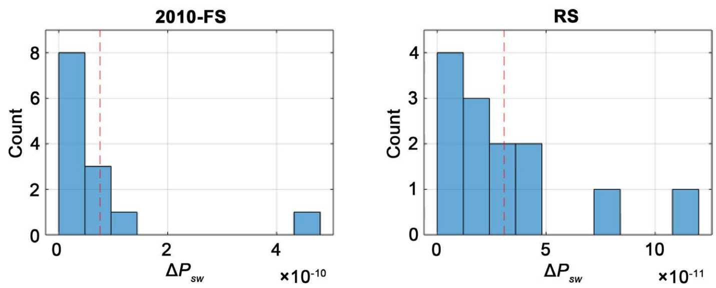

(c)

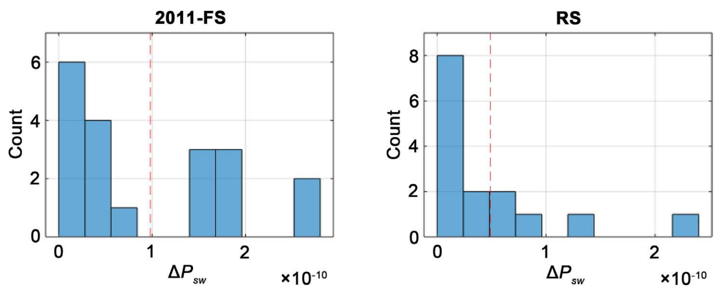

(d)

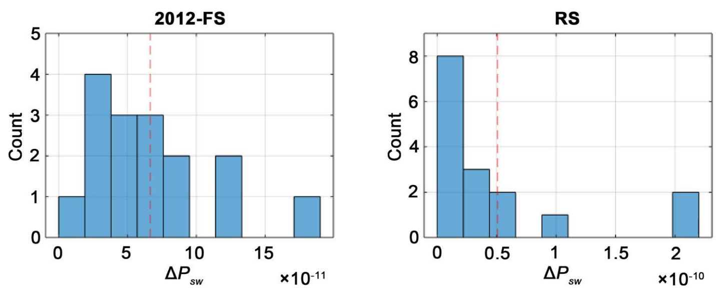

(e)

Figure 6. Dynamic pressure analysis from 2008 to 2012. Histograms of ΔP_{sw} in FS and RS shocks, the red dotted line shows the mean value in each distribution.

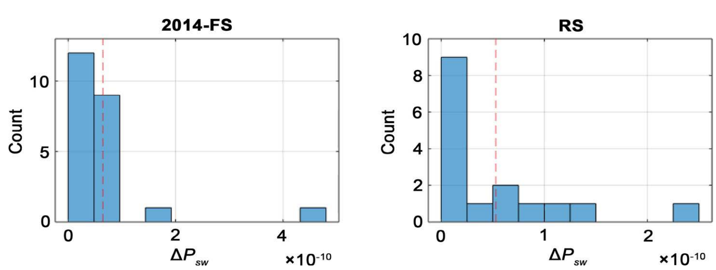

(a)

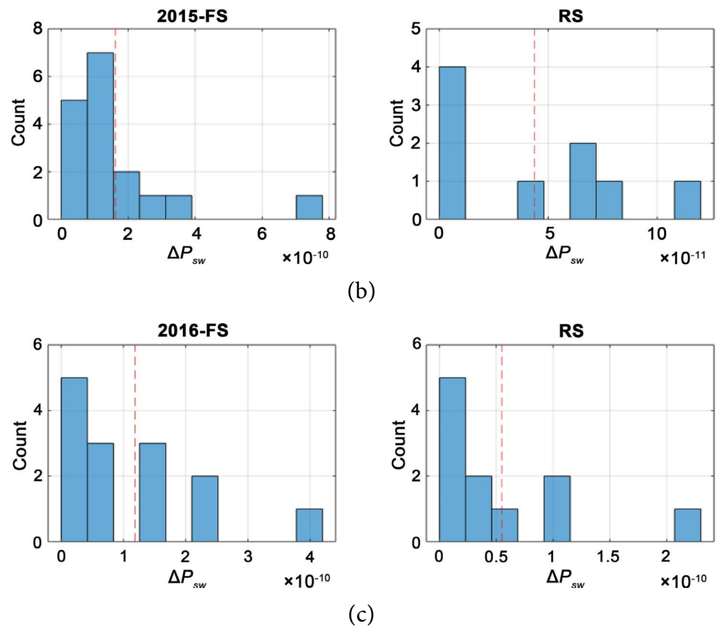

Figure 7. Dynamic pressure analysis from 2014 to 2016. Histograms of ΔP_{sw} in FS and RS shocks, the red dotted line shows the mean value in each distribution.

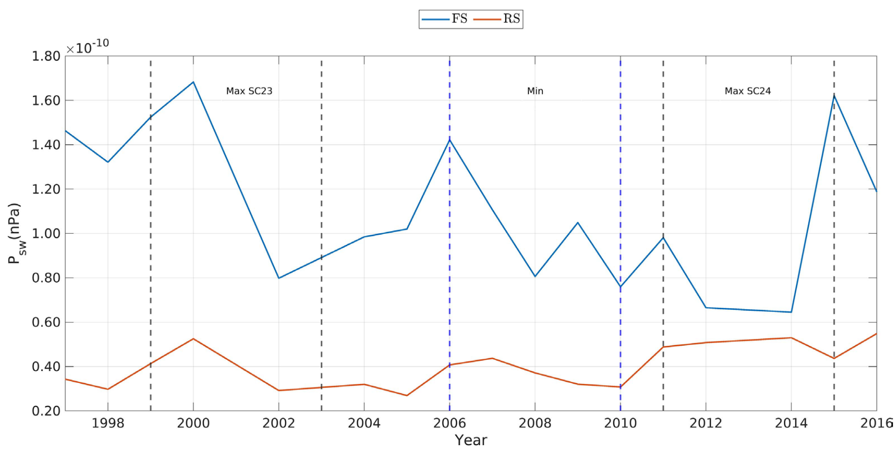

Figure 8. Mean dynamic pressure variation in time from 1997 to 2016. Dotted vertical lines denote the intervals corresponding to the maximum of solar cycles 23 and 24 and the minimum between them.

- Five hundred fifteen shocks were obtained from 1997 to 2016 during opposition periods. 58.5% corresponds to fast forward (FS) shocks, and 41.5% are fast reverse (RS) shocks (**Table 2**).
- The fast forward (FS) shocks were predominant from 1997 to 2016. As well as the dynamic pressure in fast forward shock (FS) during solar cycles 23 and 24. It can imply that the magnetospheric disturbance caused by FS shocks is considerably higher than RS shocks. It is related to the intrinsic characteristics of FS shocks because all physical quantities such as velocity, magnetic field, density, and temperature increase in time increasing the dynamic pressure.

Table 2. Interplanetary fast forward and reverse shocks from 1997 to 2016.

Year	Fast Forward Shocks (FS)	Fast Reverse Shocks (RS)	Total
1997	16	14	30
1998	13	12	25
1999	16	13	29
2000	18	11	29
2002	19	9	28
2004	19	12	31
2005	19	10	29
2006	20	14	34
2007	16	12	28
2008	17	13	30
2009	26	14	40
2010	13	13	26
2011	19	15	34
2012	16	16	32
2014	23	16	39
2015	17	9	26
2016	14	11	25
Total	301	214	515

- The relationship between the solar cycle, fast forward, and reverse shocks is summarized in **Figure 7**. In general, both kinds of shocks follow the solar cycle. FS shocks show a high value on the maximum of solar cycle 23 compared to the maximum of solar cycle 24. However, RS shocks show a similar behavior during the maximum solar cycles 23 and 24.
- An important aspect is correlating the solar wind features and the in-situ measurements in Jupiter's magnetosphere. It was explored before by Vogt *et al.* 2019 [6] using Galileo data during orbit E16 and C9 and mSWim data. These periods show a good agreement between the magnetospheric compression and the high solar wind dynamic pressure. The idea is to extend this analysis using in-situ data from other missions and describe the impact of solar wind in the planetary's magnetosphere.
- Jupiter is a complex system; e.g., internal sources such as Io mainly control the auroral radio and UV emissions, but the solar wind influence can be considered in that kind of emissions to understand their effect. As well as the correlation between solar wind pressure at Jupiter's magnetosphere and the intensity of the auroral radio emission (e.g., using the Nancay array) can help to understand the relationship between the solar wind and Jupiter's auroral dynamics. Additionally, a study about the Solar Energetic Particles (SEPs) reaching Jupiter's magnetosphere is very valuable to evaluate their influence.

Acknowledgements

J. M. R. G. thanks Ezequiel Echer for the fruitful discussions. This work was supported by NASA Goddard Space Flight Center through Cooperative Agreement 80NSSC21M0180 to Catholic University, Partnership for Heliophysics and Space Environment Research (PHaSER).

Conflicts of Interest

The author declares no conflicts of interest regarding the publication of this paper.

References

[1] Rodríguez Gómez, J.M. (2021) The Sun's Influence on Earth and Other Planets: Space Weather. *Revista Brasileira de Ensino de Física*, **43**, e20200495. https://doi.org/10.1590/1806-9126-rbef-2020-0495

[2] Plainaki, C., Lilensten, J., Radioti, A., Andriopoulou, M., Milillo, A., Nordheim, T., Dandouras, J., Coustenis, A., Grassi, D., Manganoetal, V., *et al*. (2016) Planetary Space Weather: Scientific Aspects and Future Perspectives. *Journal of Space Weather and Space Climate*, **6**, Article No. A31. https://doi.org/10.1051/swsc/2016024

[3] Bunce, E.J., Cowley, S.W.H. and Yeoman, T.K. (2004) Jovian Cusp Processes: Implications for the Polar Aurora. *Journal of Geophysical Research*: *Space Physics*, **109**, Article No. A09S13. https://doi.org/10.1029/2003JA010280

[4] Cowley, S.W.H., Badman, S.V., Imber, S.M. and Milan, S.E. (2008) Comment on "Jupiter: A Fundamentally Different Magnetospheric Interaction with the Solar Wind" by D.J. McComas and F. Bagenal. *Geophysical Research Letters*, **35**, Article No. L101010. https://doi.org/10.1029/2007GL032645

[5] McComas, D.J. and Bagenal, F. (2007) Jupiter: A Fundamentally Different Magnetospheric Interaction with the Solar Wind. *Geophysical Research Letters*, **34**, Article No. L20106. https://doi.org/10.1029/2007GL031078

[6] Vogt, M.F., Gyalay, S., Kronberg, E.A., Bunce, E.J., Kurth, W.S., Zieger, B. and Tao, C. (2019) Solar Wind Interaction with Jupiter's Magnetosphere: A Statistical Study of Galileo *in Situ* Data and Modeled Upstream Solar Wind Conditions. *Journal of Geophysical Research*: *Space Physics*, **124**, 10170-10199. https://doi.org/10.1029/2019JA026950

[7] Brice, N.M. and Ioannidis, G.A. (1970) The Magnetospheres of Jupiter and Earth. *Icarus*, **13**, 173-183. https://doi.org/10.1016/0019-1035(70)90048-5

[8] Delamere, P.A. and Bagenal, F. (2010) Solar Wind Interaction with Jupiter's Magnetosphere. *Journal of Geophysical Research*, **115**, Article No. A10201. https://doi.org/10.1029/2010JA015347

[9] Badman, S.V., Bonfond, B., Fujimoto, M., Gray, R.L., Kasaba, Y., Kasahara, S., Kimura, T., Melin, H., Nichols, J.D., Steffl, A.J., Tao, C., Tsuchiya, F., Yamazaki, A., Yoneda, M., Yoshikawa, I. and Yoshioka, K. (2016) Weakening of Jupiter's Main Auroral Emission during January 2014. *Geophysical Research Letters*, **43**, 988-997. https://doi.org/10.1002/2015GL067366

[10] Dunn, W.R., Branduardi-Raymont, G., Elsner, R.F., Vogt, M.F., Lamy, L., Ford, P.G., Coates, A.J., Gladstone, G.R., Jackman, C.M., Nichols, J.D., Rae, I.J., Varsani, A., Kimura, T., Hansen, K.C. and Jasinski, J.M. (2016) The Impact of an ICME on the Jovian X-Ray Aurora. *Journal of Geophysical Research*: *Space Physics*, **121**, 2274-2307. https://doi.org/10.1002/2015JA021888

[11] Panchenko, M., Rucker, H.O. and Farrell, W.M. (2013) Periodic Bursts of Jovian Non-Io Decametric Radio Emission. *Planetary and Space Science*, **77**, 3-11. https://doi.org/10.1016/j.pss.2012.08.015

[12] Hess, S.L.G., Echer, E. and Zarka, P. (2012) Solar Wind Pressure Effects on Jupiter Decametric Radio Emissions Independent of Io. *Planetary and Space Science*, **70**, 114-125. https://doi.org/10.1016/j.pss.2012.05.011

[13] Echer, E., Zarka, P., Gonzalez, W.D., Morioka, A. and Denis, L. (2010) Solar Wind Effects on Jupiter Non-Io DAM Emissions during Ulysses Distant Encounter (2003-2004). *Astronomy and Astrophysics*, **519**, Article No. A84. https://doi.org/10.1051/0004-6361/200913305

[14] Nichols, J.D., Clarke, J.T., Gérard, J.C., Grodent, D. and Hansen, K.C. (2009) Variation of Different Components of Jupiter's Auroral Emission. *Journal of Geophysical Research*, **114**, Article No. A06210. https://doi.org/10.1029/2009JA014051

[15] Chané, E., Saur, J., Keppens, R. and Poedts, S. (2017) How Is the Jovian Main Auroral Emission Affected by the Solar Wind? *Journal of Geophysical Research*: *Space Physics*, **122**, 1960-1978. https://doi.org/10.1002/2016JA023318

[16] Zarka, P. (1998) Auroral Radio Emissions at the Outer Planets: Observations and Theories. *Journal of Geophysical Research*, **103**, 20159-20194. https://doi.org/10.1029/98JE01323

[17] Zieger, B. and Hansen, K.C. (2008) Statistical Validation of a Solar Wind Propagation Model from 1 to 10 AU. *Journal of Geophysical Research*: *Space Physics*, **113**, Article No. A08107. https://doi.org/10.1029/2008JA013046

[18] Tóth, G. (1996) A General Code for Modeling MHD Flows on Parallel Computers: Versatile Advection Code. *Astrophysical Letters and Communications*, **34**, 245-250.

[19] Hess, S.L.G., Echer, E., Zarka, P., Lamy, L. and Delamere, P.A. (2014) Multi-Instrument Study of the Jovian Radio Emissions Triggered by Solar Wind Shocks and Inferred Magnetospheric Subcorotation Rates. *Planetary and Space Science*, **99**, 136-148. https://doi.org/10.1016/j.pss.2014.05.015

[20] Echer, E. (2019) Interplanetary Shock Parameters near Jupiter's Orbit. *Geophysical Research Letters*, **46**, 5681-5688. https://doi.org/10.1029/2019GL082126

[21] Rodríguez-Gómez, J.M., Podladchikova, T., Veronig, A., Ruzmaikin, A., Feynman, J. and Petrukovich, A. (2020) Clustering of Fast Coronal Mass Ejections during Solar Cycles 23 and 24 and the Implications for CME-CME Interactions. *The Astrophysical Journal*, **899**, Article No. 47. https://doi.org/10.3847/1538-4357/ab9e72

[22] Ebert, R., Bagenal, F., McComas, D. and Fowler, C. (2014) A Survey of Solar Wind Conditions at 5 AU: A Tool for Interpreting Solar Wind-Magnetosphere Interactions at Jupiter. *Frontiers in Astronomy and Space Sciences*, **1**, Article 4. https://doi.org/10.3389/fspas.2014.00004

Appendix 1

Interplanetary fast shocks covering the period described above.

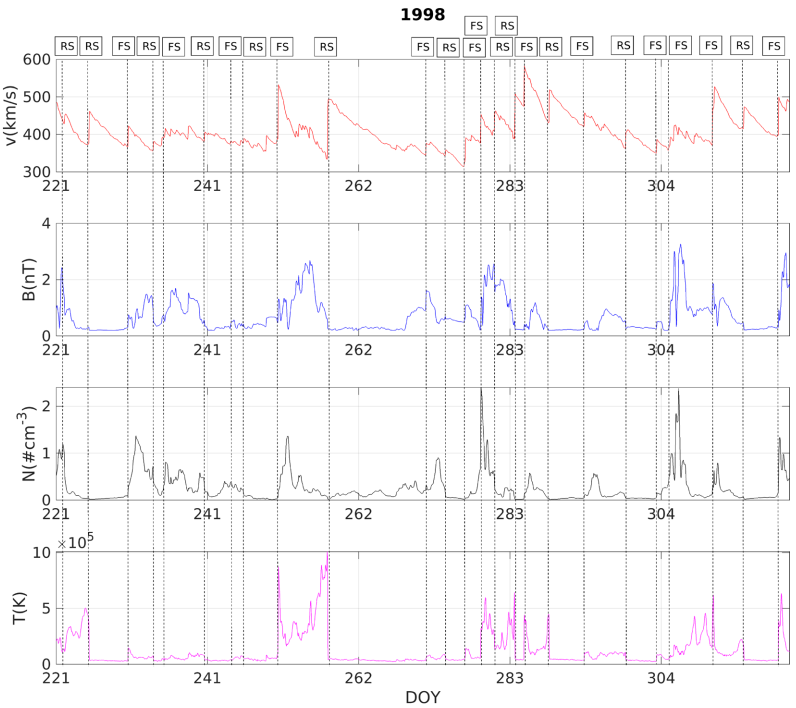

Figure A1. Solar wind data from mSWim from 221 to 321 DOY 1998. From upper to lower panel: solar wind speed (v), magnetic field magnitude (B), density (N) and Temperature (T). Dotted vertical lines indicate the interplanetary shocks FS and RS.

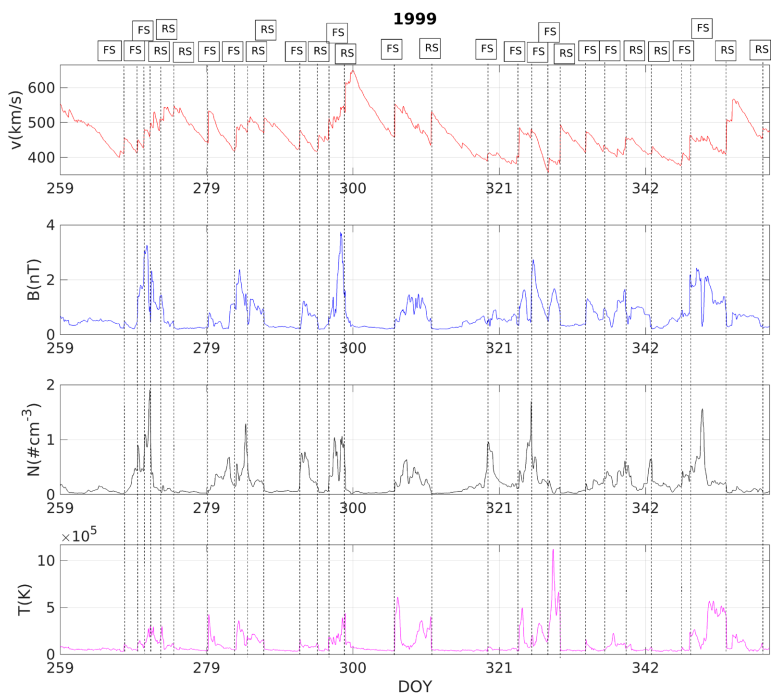

Figure A2. Solar wind data from mSWim from 221 to 321 DOY 1999.

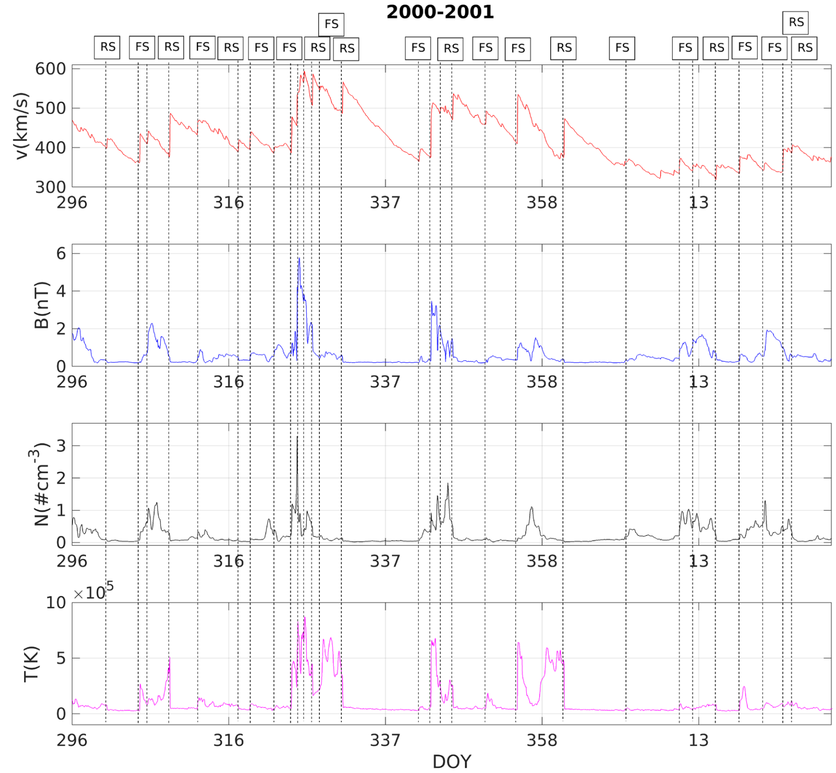

Figure A3. Solar wind data from mSWim from 296 DOY 2000 to 31 DOY 2001.

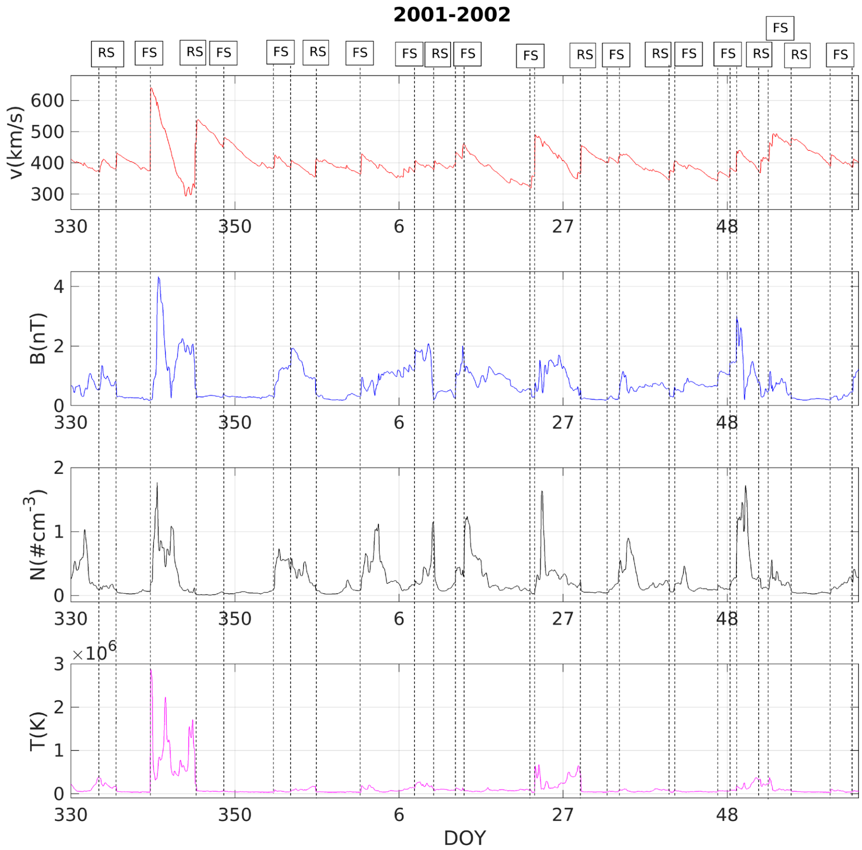

Figure A4. Solar wind data from mSWim from 330 DOY 2001 to 64 DOY 2002.

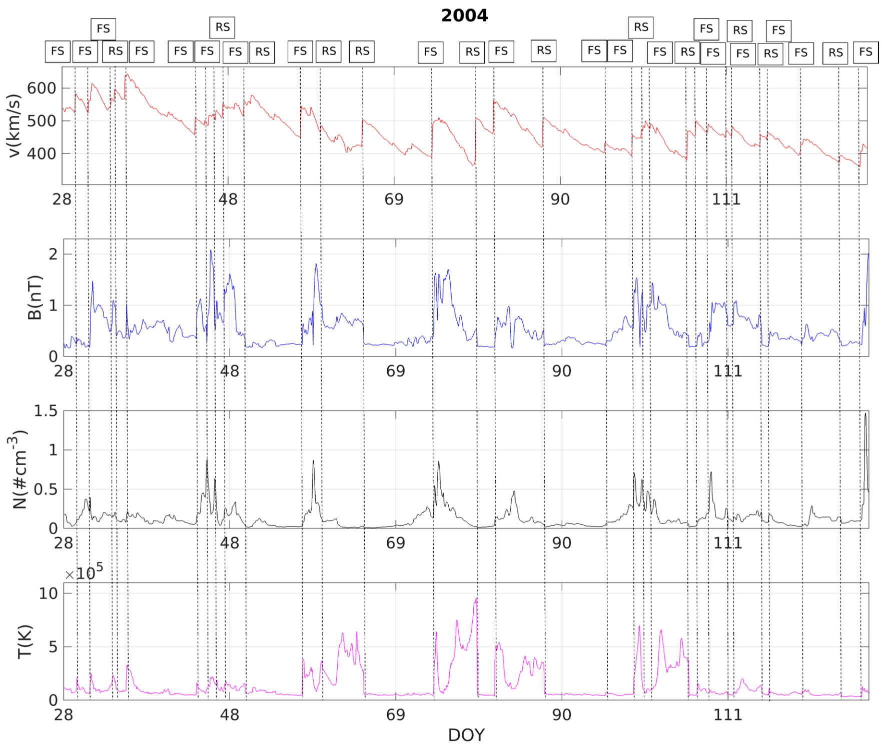

Figure A5. Solar wind data from mSWim from 28 to 128 DOY 2004.

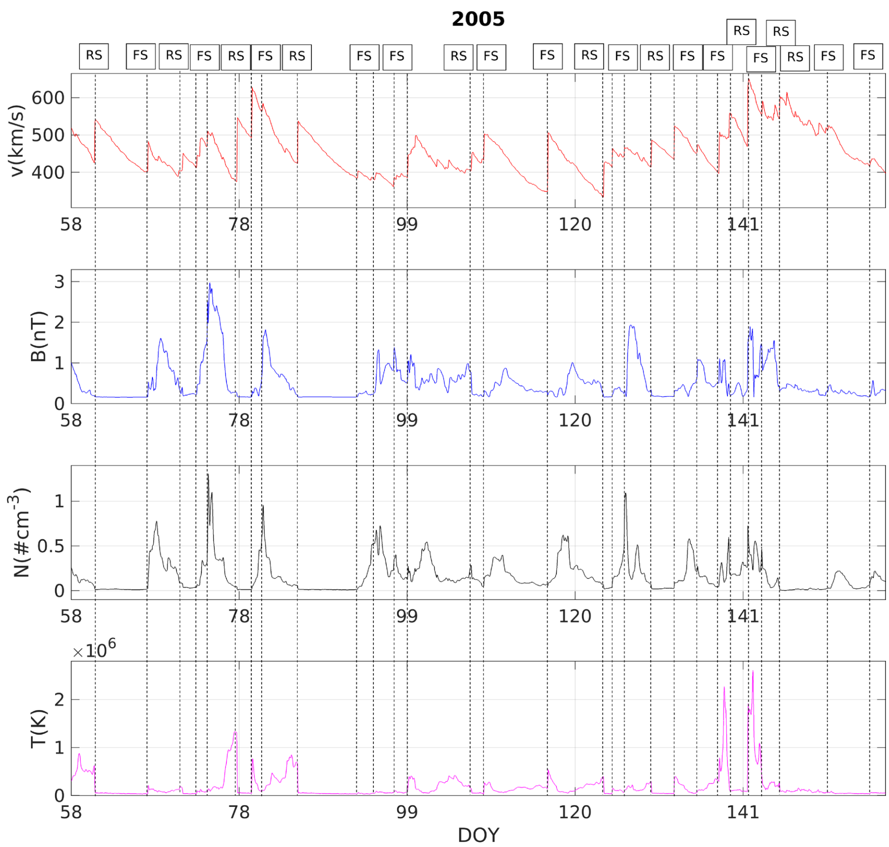

Figure A6. Solar wind data from mSWim from 58 to 158 DOY 2005.

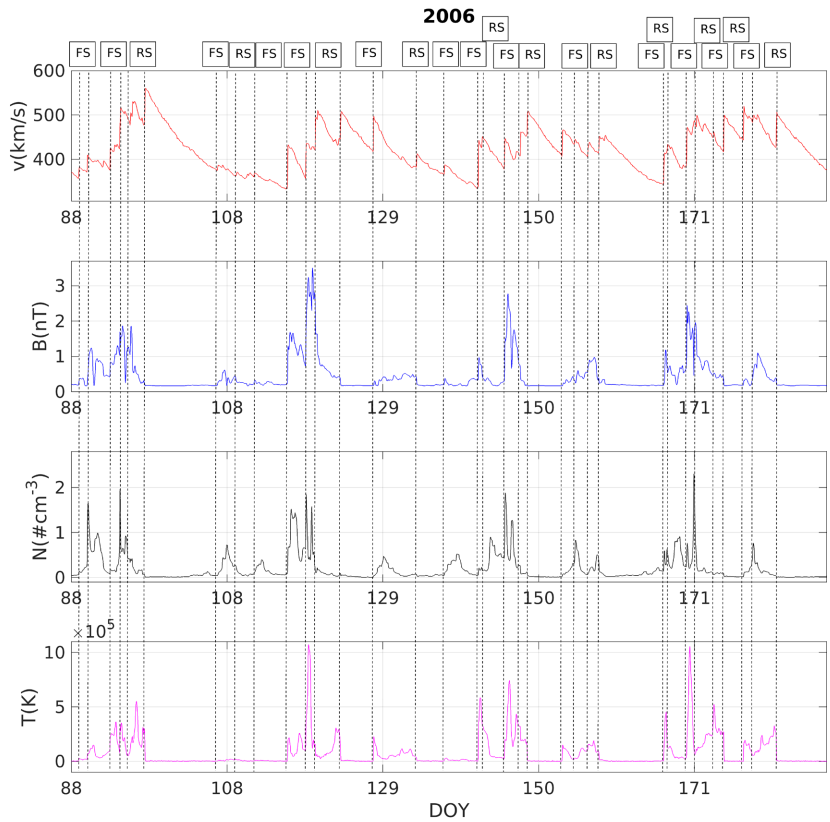

Figure A7. Solar wind data from mSWim from 88 to 188 DOY 2006.

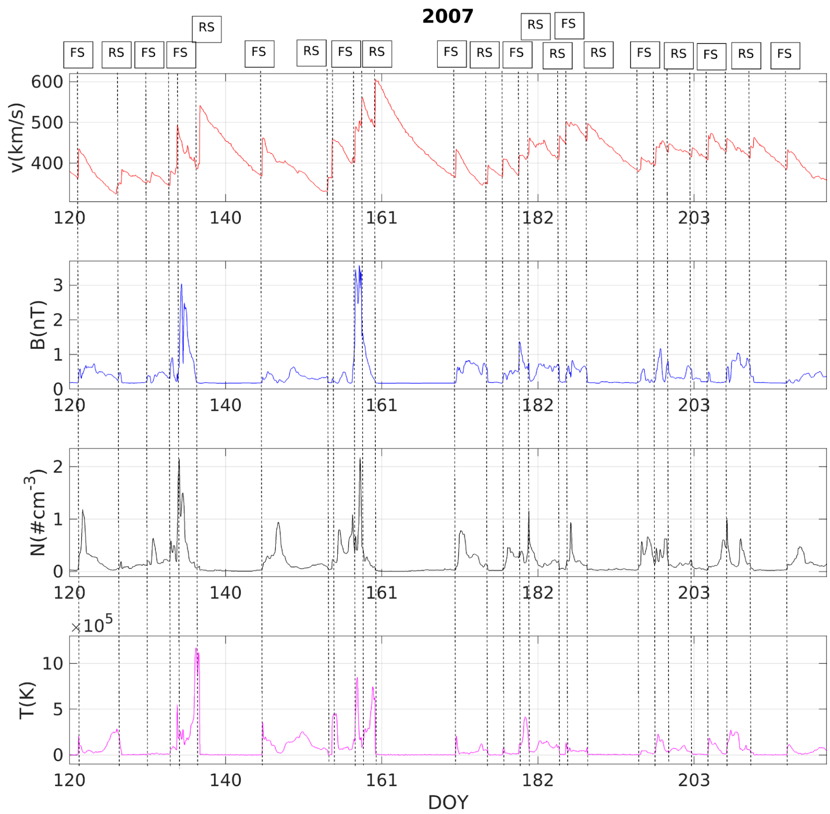

Figure A8. Solar wind data from mSWim from 120 to 220 DOY 2007.

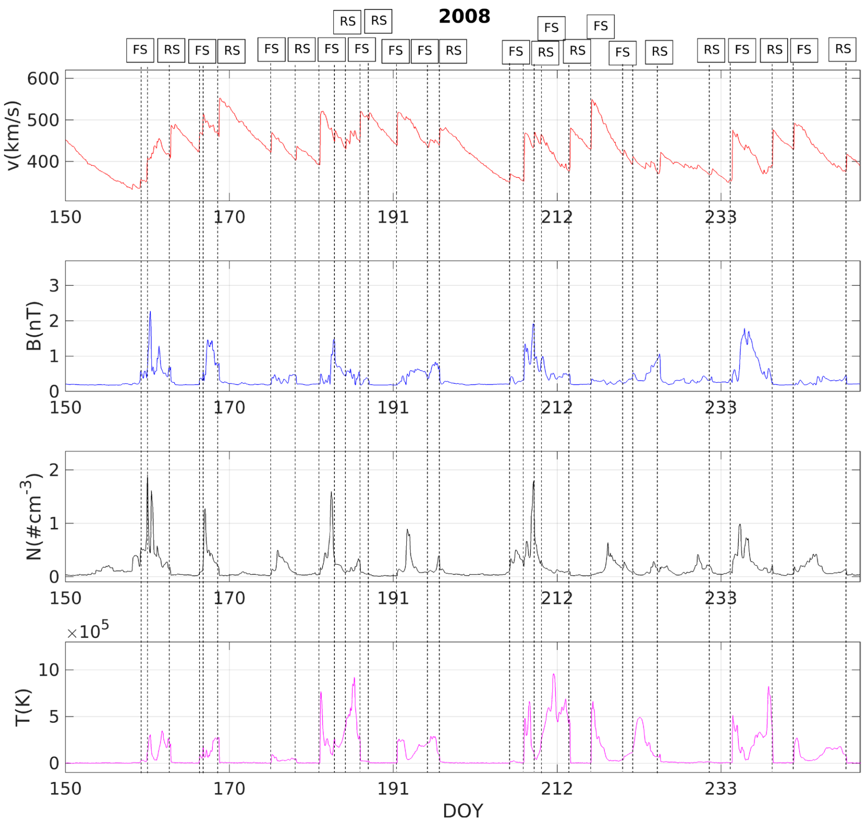

Figure A9. Solar wind data from mSWim from 150 to 254 DOY 2008.

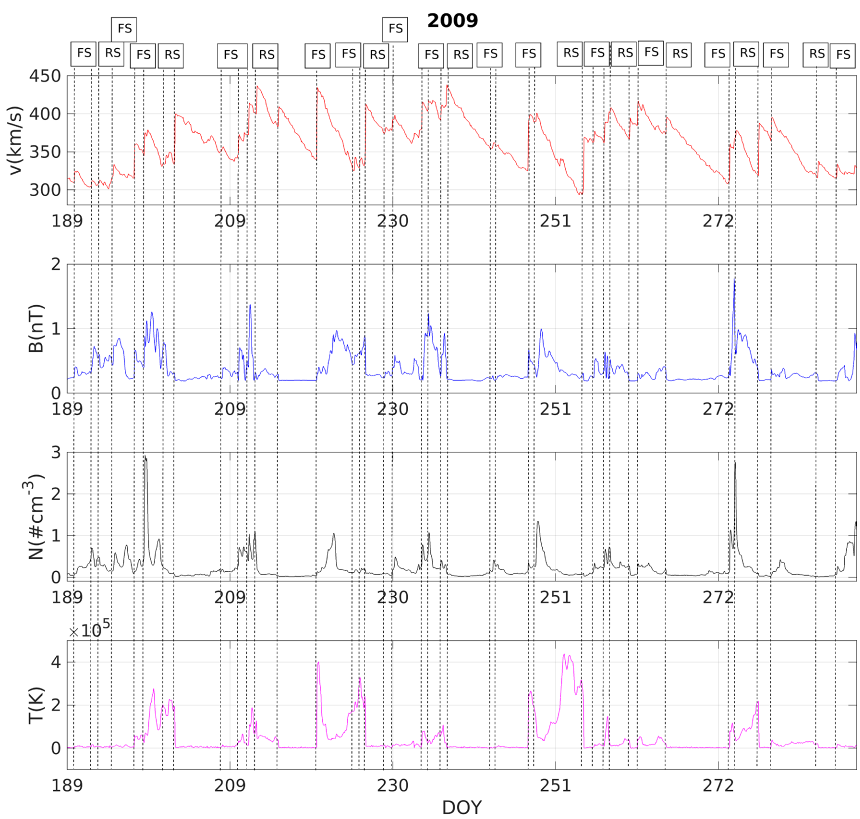

Figure A10. Solar wind data from mSWim from 189 to 289 DOY 2009.

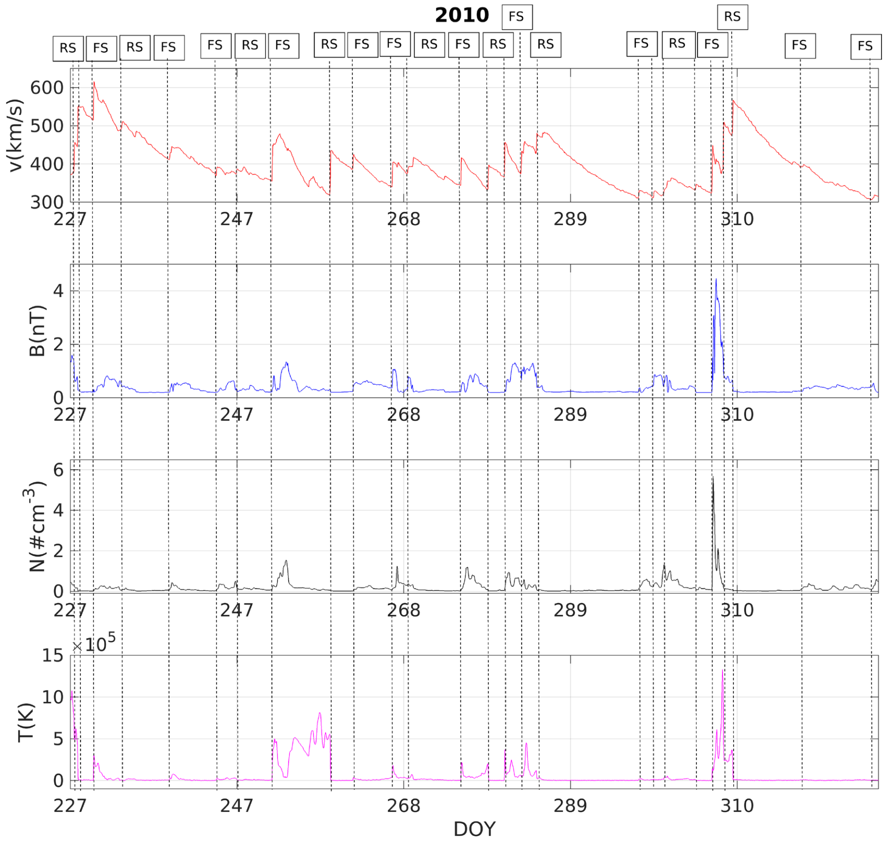

Figure A11. Solar wind data from mSWim from 227 to 327 DOY 2010.

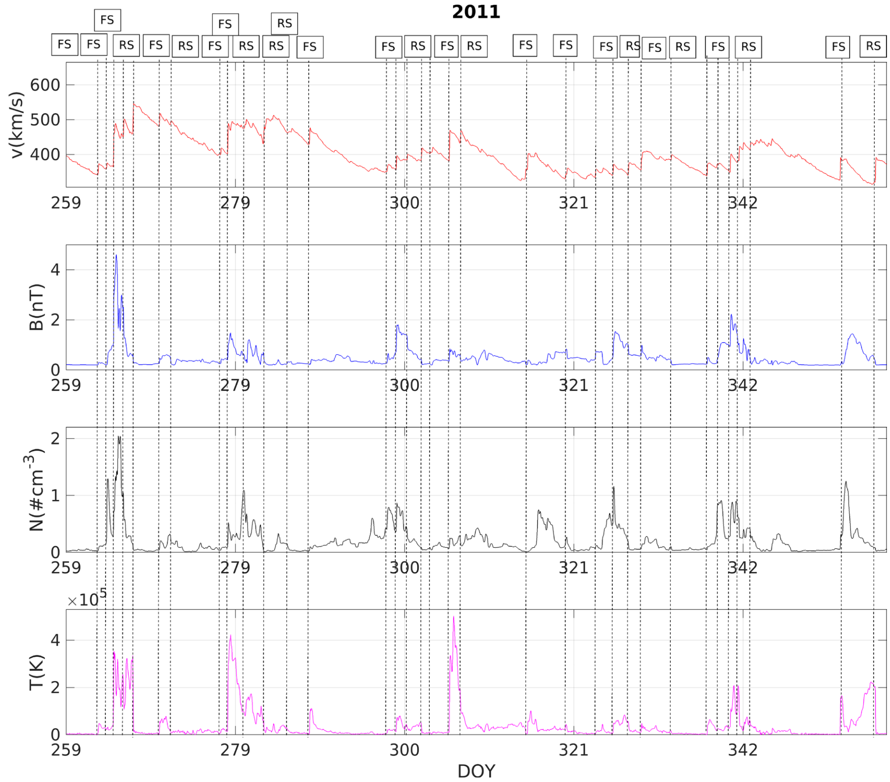

Figure A12. Solar wind data from mSWim from 264 to 364 DOY 2011.

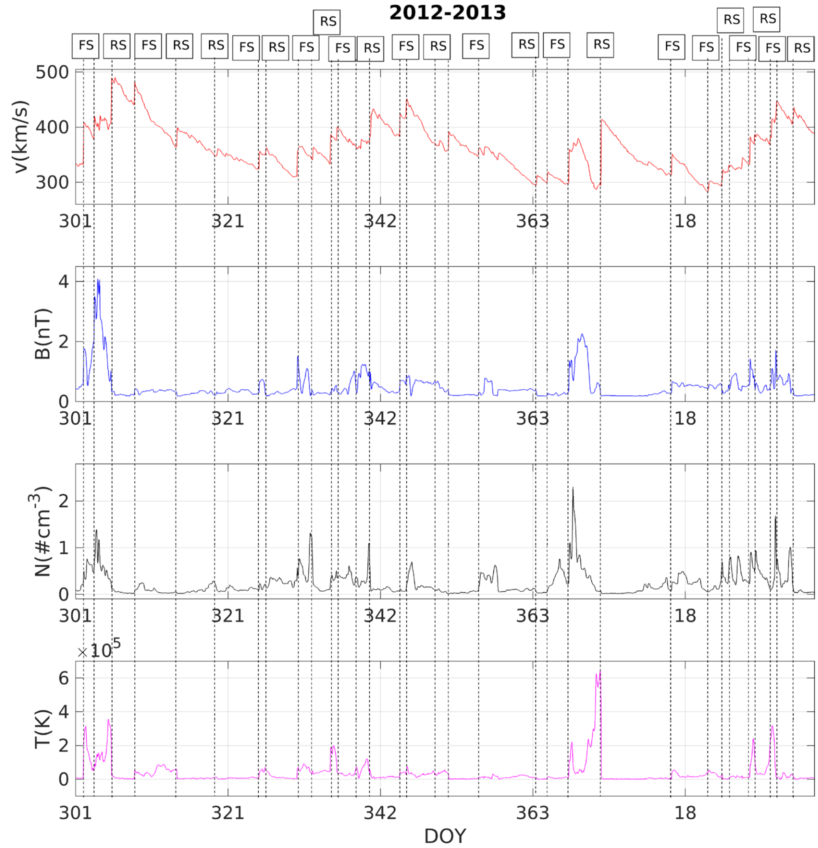

Figure A13. Solar wind data from mSWim from 301 DOY 2012 to 35 DOY 2013.

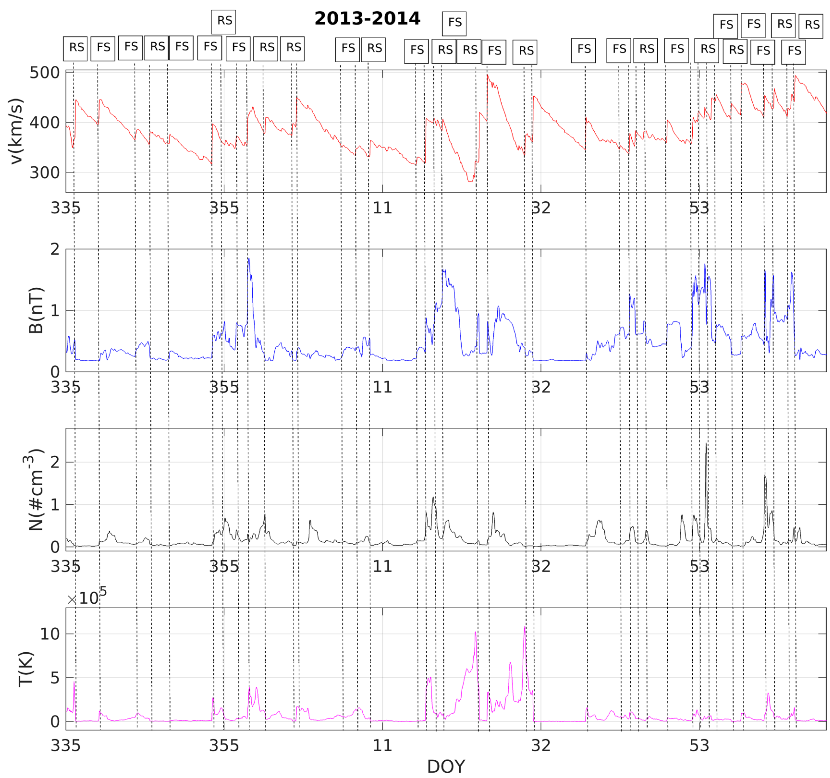

Figure A14. Solar wind data from mSWim from 335 DOY 2013 to 69 DOY 2014.

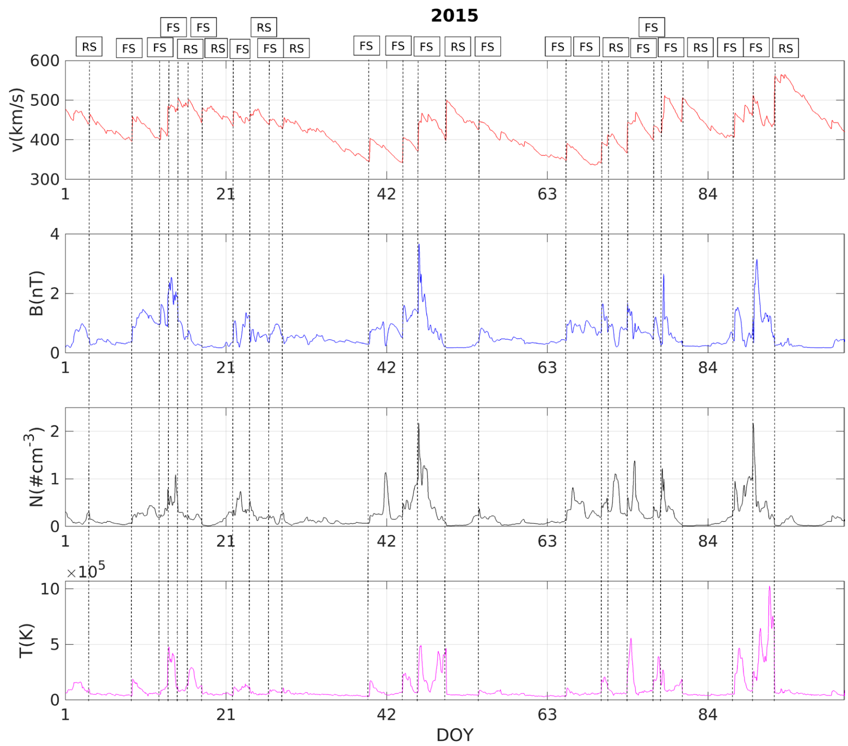

Figure A15. Solar wind data from mSWim from 1 to 101 DOY 2015.

Appendix 2

Detailed information about FS and RS shocks from 1997 to 2016. Initial and final shock time (hrs), DOY, shock type, the $\Gamma_B = B_2/B_1$, $\Gamma_N = N_2/N_1$, where B_2 and N_2 are the magnetic field and density after shock, B_1 and N_1 is the magnetic field and density before shock. Details see: https://we.tl/t-x3iN9LFfUc.